Numerical Analysis of the structural response of RC-framed buildings subjected to internal explosions

M.A. Zanini, P. Mocellin, C. Vianello, G. Maschio
University of Padova, Department of Industrial Engineering, Padua, Italy

F. Faleschini, M. Andreotti, C. Pellegrino, C. Modena
University of Padova, Department of Civil, Environmental and Architectural Engineering, Padua, Italy

ABSTRACT: Internal gas explosions can lead to structural failures which seriously compromises the static of a building, both in civil and industrial structures, and in some cases can involve the consequent entire structure' failure. The main purpose of this paper is to numerically reproduce the damage effects caused by a vented explosion in a multi-storey framed reinforced concrete structure with masonry infill walls. ANSYS AUTODYN® has been used to manage both the structural (Lagrangian solver) and the fluid-dynamic (Eulerian solver) issues and to make feasible their interactions. The analysis focuses on the gas mixture usually used for domestic purposes mainly consisting by methane (80 % v/v) and completed by ethane, propane and n-butane. In conclusion, applying corrects material properties and the analyzed pressure wave, the focus is on the damages of structure.

1 INTRODUCTION

Recent explosions due to a gas leak are very frequent in Italy, they cause death and a huge damage in structures under blast load. As example, for gas-leakage, in pipes of residential plants, 177 incidents occurred in 2012, 144 in 2011 and 200 in 2009-2010. So the actual technical normative and the fabrication of devices and components aren't enough to eliminate the issue. This paper aims to present a study for the estimation of the peak pressure induced in a residential building room by a gas-leakage.

2 EXPLOSION CHEMISTRY

The mixture considered in this study can be characterized by the composition reported in Table 1 matching that generally used for domestic purposes. Compounds properties are derived from Green et al., 2008.

Table 1. Gas mixture composition.

Compound	Fraction	$\Delta_f G_i^0$ [kJ mol^{-1}]
Methane	0.8	-50.5
Ethane	0.08	-32.0
Propane	0.06	-23.4
Butane	0.06	-17.0

Given the thermodynamic conditions of the system, it is supposed to behave as a mixture of ideal gases starting from an initial state characterized by an atmospheric pressure and a temperature of 273 K. The thermochemical description of the domain is primarily linked to the evaluation of the maximum energy released with the reaction. The calculation has been achieved by implementing a stoichiometric reaction scheme in the gas phase that leads to the following overall reaction:

$$CH_{1.38}H_{4.76} + 3.76(O_2 + 3.76N_2) \rightarrow 1.38CO_2 + +2.38H_2O + 14.1376N_2 \quad (1)$$

The maximum energy expresses in terms of mechanical work W is therefore obtained considering a isochoric and adiabatic path. Assuming that vapors form ideal solutions since the contribution of the solution non-ideality to the energy is small compared with the chemical reaction term, it is possible to derive the following expression:

$$W = G^f(T^f, P^f, n^f) - G^i(T^i, P^i, n^i) - RT(n_{tot}^f - n_{tot}^i) \quad (2)$$

where G stands for the Gibbs free energy, n for the number of moles while the superscripts i, f are referred respectively to the initial and final state. In Equation (2) the total specific Gibbs free energy should consider the variation in the number of mole through the reaction as:

$$G(T,P,n) = \sum_{NC,i} n_i \bar{G}_i(T,P,x) =$$

$$= \sum_{NC,i} n_i \left(\Delta_f \overline{G_i^0} + RT \ln x_i\right) \quad (3)$$

The application of these approach leads to the estimation of the total work that can be extracted from the system and equals to -4.49E+04 kJ kg^{-1}. The TNT equivalency amounts to about 24 kg considered a value for the TNT heat of decomposition of -4570 kJ kg^{-1} (Whittaker and Sherkar 2010) that has then been scaled.

3 NUMERICAL MODELING

The model is composed of the room and air volume occupied by the building. A 3D Euler FCT (higher order Euler processor) sub grid was used for the air. The ground level was supposed rigid and air flow out was considered in the rest of the borders.
The structure model was composed of the reinforced concrete structure and masonry infill walls. A rigid floor of the underground level was used to simulate the soil. The reinforced concrete structure was a frame structure composed by columns, beams and slabs.
The mesh is discretized greater for Eulerian elements to better describe the trend spherical expansion of the detonation and to have pressure results similar to those which would be found in reality, while larger mesh are used for the elements Lagrangian.
Columns, beams and slabs were modeled with 3D solid elements that were solved with a Lagrange processor. Walls in the room were filled in masonry walls, they were modeled as perfectly joined to the reinforced concrete frame. All the individual parts are connected to each other through bonded contact surfaces. This type of connections between masonry and frame it's the worst situation that can be encountered, providing a greater degree of confinement, despite cushioning elements in this configuration assume a behavior to the plate thus increasing the maximum stresses tolerable.
The mechanical properties of the different parts of the model are described in the following. Lagrange elements were used for the structural part whereas Euler elements for fluid part. The initial boundary conditions were defined by atmospheric pressure and environmental temperature. The part of the fluid also extends to a meter externally to the walls of the room, allowing a detection of the correct pressures at the Gauges points even in the case of high strain of structural elements. At this part was set a flowout boundary condition to the top and lateral sides to allow the spillage of the blast load wave without incurring in no real reflection waves.
With the use of an explicit solver the mesh was designed to be as regular as possible, avoiding excessive deformations of each mesh.
The mesh size for Lagrange elements was supposed of 200 mm and for Euler elements of 3.7 mm.

4 MATERIALS

4.1 *Air*

Air is a gas and for this it isn't necessary modeling resistance and failure patterns. Just setting the equation of state of ideal gases in the form:

$$p = (\gamma - 1)\rho e \tag{4}$$

where γ is the adiabatic constant, ρ is the air density and e is the specific internal energy. The latter is $2.068 \cdot 10^5 J/kg$ and its varying in function of the temperature with the formula:

$$\mathrm{e} = \frac{\mathrm{RT}}{\gamma - 1} \tag{5}$$

where $R = 287.1 \frac{J}{kgK}$ is the gas constant, $\gamma = 1.4$ and T it considers a temperature of 288.15 K.

4.2 *TNT*

Explosives are modeled with the equation of state for explosive products defined by the empirical equation JWL. These are implemented in many hydrocodes (for example LS-DYNA, AUTODYN) and have the following form:

$$p = A\left(1 - \frac{\omega}{R_1 V}\right)e^{-R_1 V} + B\left(1 - \frac{\omega}{R_2 V}\right)e^{-R_2 V} + \frac{\omega E}{V} \tag{6}$$

where the coefficients A, B, R_1, R_2 and ω depend on the composition of the explosive, the variable $V = v/v_0$ is the expansion of the explosive products and E the detonation energy per volume unit. The most used explosive substances were reported in the Autodyn library (Table 2). For the TNT case, when the expansion of the explosive products reaches 10 times the starting volume was set the transformation of the equation of state from JWL to ideal gas.

Table 2. TNT Equation of State Parameters.

Parameter	Value
Density	1,630
A (GPa)	371.2
B (GPa)	3.231
R_1	4.15
R_2	0.95
Adiabatic constant, ω	0.30
Detonation velocity, D (m/s)	6,930
Energy per unit volume, E_0 (GPa)	7
CJ pressure, P_{CJ} (GPa)	21

At the beginning the blast load was implemented with 1D wedge (Figure 1) to allow wave's development until the encounter with the first wall at a high computational velocity.
Chemical properties and stechiometric conditions determinate the equivalent TNT mass that cause the blast load in the model. It is indicated in Table 3.

Table 3. TNT-LPG Equivalency.

Substance	Mass (kg)
LPG	2.30
TNT	0.72

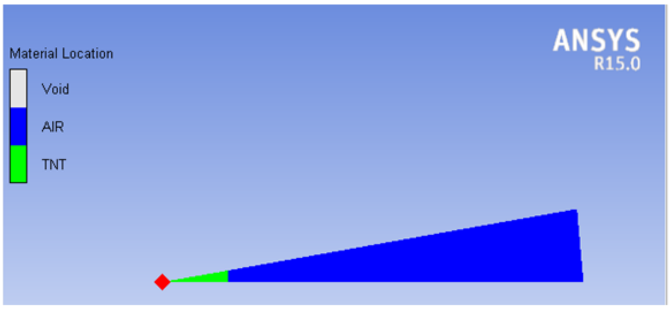

Figure 1. Implementation of TNT 1D on AUTODYN

4.3 *Reinforced Concrete*

The equation of state consider the pressure p a function of density ρ with an approximation of Hook's law in the following manner:

$$p = K\mu \tag{7}$$

where $\mu = \left(\frac{\rho}{\rho_0}\right) - 1$ is the compression, ρ_0 is the reference density and K is the Bulk Modulus of the material. Reinforced concrete elements can be modeled as a combination of joined elements of concrete and steel with the assumption of perfect contact.
It was decided to use an homogenized elastic-plastic material to simulate the behavior of reinforced concrete presents in columns, beams and slabs. The section for both pillars that for beams was considered of 30x30 cm with an armature equal to 1% of the area.
The tensile strength was considered like the steel strength and compressive strength as concrete. It was considered also the increase of the mechanical properties due to high strain rate. The law has been studied in CEB Model Code 2010 which can describe the variations in compressive, tensile strength and in elastic modulus. Quasi-static strain rate is on order of $10^{-6}\ s^{-1}$ and with big explosions the strain rate is on order of $10^{-3} s^{-1}$.
For compressive strength that can be used the follow relations (fib, 2013):

$$f_{cm}^{dyn} = f_{cm}\left(\frac{\dot{\varepsilon_c}}{\dot{\varepsilon_{c0}}}\right)^{0.014} \quad per\ \dot{\varepsilon_c} \leq 30s^{-1} \tag{8}$$

$$f_{cm}^{dyn} = f_{cm} \cdot 0.012 \cdot \left(\frac{\dot{\varepsilon_c}}{\dot{\varepsilon_{c0}}}\right)^{\frac{1}{3}} \quad per\ \dot{\varepsilon_c} > 30s^{-1} \tag{9}$$

With $\dot{\varepsilon_{ct0}} = 1 \cdot 10^{-6}\ s^{-1}$.

For tensile strength the following expressions (fib 2013) can be used:

$$f_{cm}^{dyn} = f_{cm}\left(\frac{\dot{\varepsilon_{ct}}}{\dot{\varepsilon_{ct0}}}\right)^{0.018} \quad per\ \dot{\varepsilon_{ct}} \leq 10s^{-1} \tag{10}$$

$$f_{cm}^{dyn} = f_{cm} \cdot 0.0062 \cdot \left(\frac{\dot{\varepsilon_{ct}}}{\dot{\varepsilon_{ct0}}}\right)^{\frac{1}{3}} \quad per\ \dot{\varepsilon_{ct}} > 10s^{-1} \tag{11}$$

con $\dot{\varepsilon_{ct0}} = 1 \cdot 10^{-6}\ s^{-1}$.

whereas for elastic modulus (fib, 2013):

$$E_{cm}^{dyn} = E_{cm}\left(\frac{\dot{\varepsilon_{ct}}}{\dot{\varepsilon_{ct0}}}\right)^{0.026} \tag{12}$$

with $\dot{\varepsilon_c} = 30 \cdot 10^{-6}\ s^{-1}$

To take account of the increase in resistance of the steel bars of reinforcement inside the structural elements in reinforced concrete, it is used the formula provided by Malvar (fib, 2013):

$$f_{yk}^{dyn} = f_{yk}\left(1 + \frac{6}{f_{yk}} \ln\left(\frac{\dot{\varepsilon_c}}{5 \cdot 10^{-5}}\right)\right) \tag{13}$$

The first simulation was implemented with material static properties and then it was repeated with updated dynamic properties corrected by DIF coefficient for high strain rate of different elements of the structure. Table 4 lists adopted reinforced concrete material properties.

Table 4. Reinforced Concrete C25/30 Properties.

Parameter	Value
Density (kg/m^3)	2,500
E_{rc} (MPa)	35,155.33
ν	0.25
G_{rc} (MPa)	14,062.13
B_{rc} (MPa)	23,436.89
Yield stress (kPa)	4,019.20
Principal tensile failure stress (kPa)	4,823.04
Max principal stress difference/2 (kPa)	6,600.00
Failure erosion model	

4.4 *Masonry*

The equation of state used for masonry is equal to that of reinforced concrete and also in this case using a homogenized material. Table 5 lists adopted masonry material properties. For the increasing of strength for high strain rate, the formula used is the following (Ming Wang, 2008):

$$DIF = c_1 + c_2 \log_{10}(\dot{\varepsilon_c}) + c_3(\log_{10}(\dot{\varepsilon_c}))^2 \tag{14}$$

where coefficients are:

- for elastic modulus

$$\leq 1.05s^{-1} \quad c_1 = 1.0460 \quad c_2 = 0.0153 \quad c_3 = 0 \tag{15}$$

$$> 1.05s^{-1} \quad c_1 = 1.0447 \quad c_2 = 0.0709 \quad c_3 = 0.3339 \tag{16}$$

- for compressive strength:

$$\leq 3.55s^{-1} \quad c_1 = 1.1140 \quad c_2 = 0.0380 \quad c_3 = 0 \tag{17}$$

$$> 3.55s^{-1} \quad c_1 = 1.1338 \quad c_2 = -0.3417 \quad c_3 = 0.6247 \tag{18}$$

- for tensile strength:

$$\leq 1.21s^{-1} \quad c_1 = 1.0600 \quad c_2 = 0.0200 \quad c_3 = 0 \tag{19}$$

$$> 1.21s^{-1} \quad c_1 = 1.0275 \quad c_2 = 0.3751 \quad c_3 = 0.3872 \tag{20}$$

Table 5. Masonry Properties.

Parameter	Value
Density (kg/m^3)	1,000
E_m (MPa)	2,046.00
ν	0.25
G_m (MPa)	818.40
B_m (MPa)	1,364.00
Yield stress (kPa)	290.00
Slope (°)	40.00
Principal tensile failure stress (kPa)	200.00
Max principal stress difference/2 (kPa)	400.00
Failure erosion model	

5 EFFECT OF THE BLAST LOAD

It was considered a confined blast load in a RC framed structure with different configurations of the infill masonry. These configurations are the most frequently in residential buildings. Numerical analyses were performed with ANSYS AUTODYN (ANSYS 2009).
In the first time it was supposed infill masonry of 30 cm in thickness. Later two of these walls was replaced with ones of 10 cm in thickness (normal partition walls). For analyzing the pressure developed in the internal room there were positioned Gauges points represented in Figure 2.

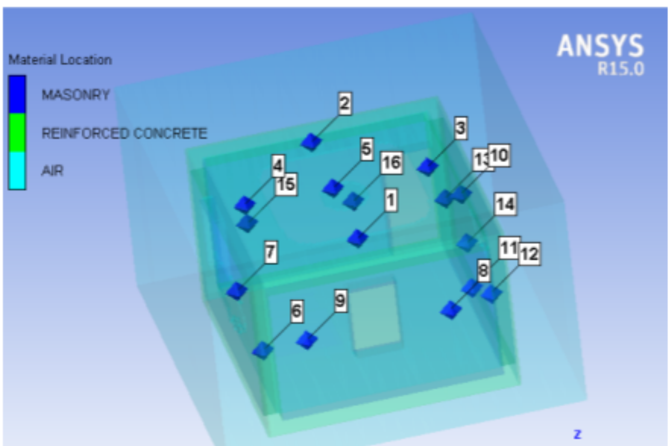

Figure 2. Gauges point location in the room.

The pressure trends developed were reported in Figure 3 differentiated by Gauges points localization.

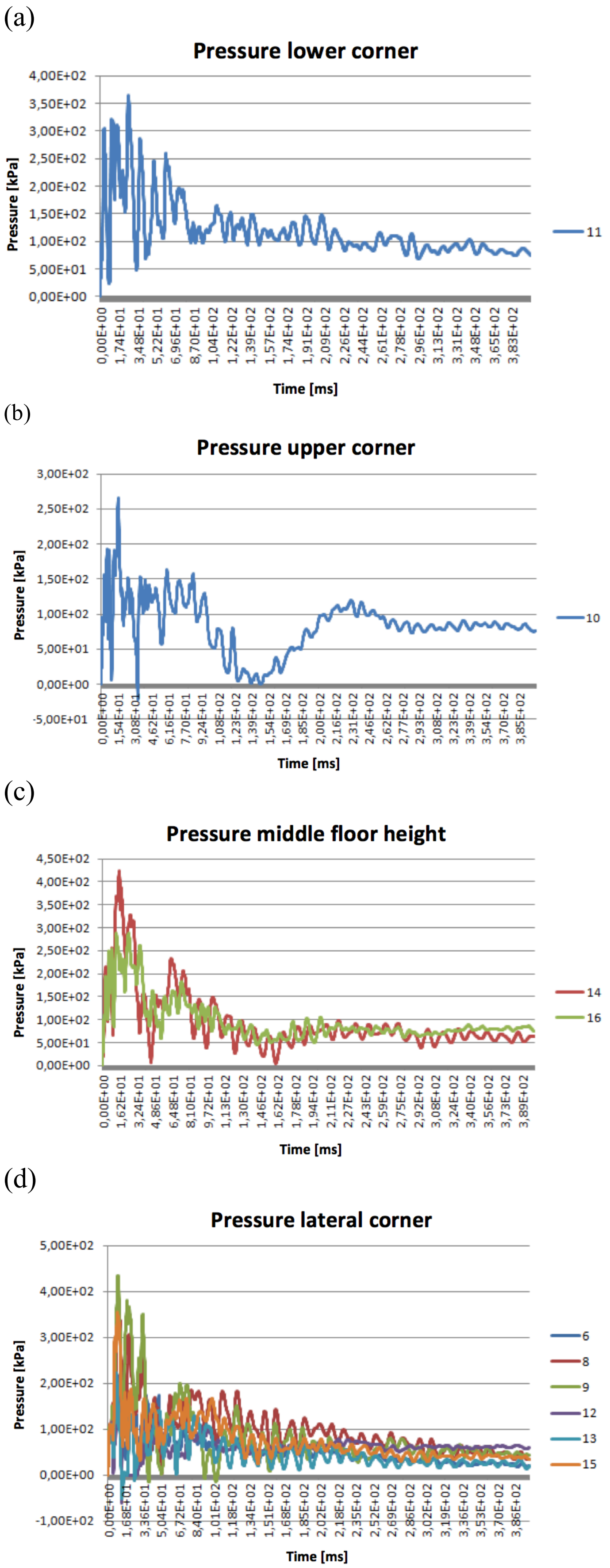

Figure 3. Pressure trend in Gauges points: room lower corner (a), upper corner (b), middle floor heigh (c) and lateral corner (d).

The upper floor presents a pressure trend very different from lateral walls because it is more subjected to reflected waves, because of the distances between ground and upper floor are smaller than distances between opposite walls of the room.
Curves reported, are comparable with a hyperbolic function: this result is in good agreement with the classic function that could be utilized to describe a detonation pressure trend.
In the first model case depressions are the dominant waves which are one and a half positive pressures.
Damages of the structure are represented in Figure 4.

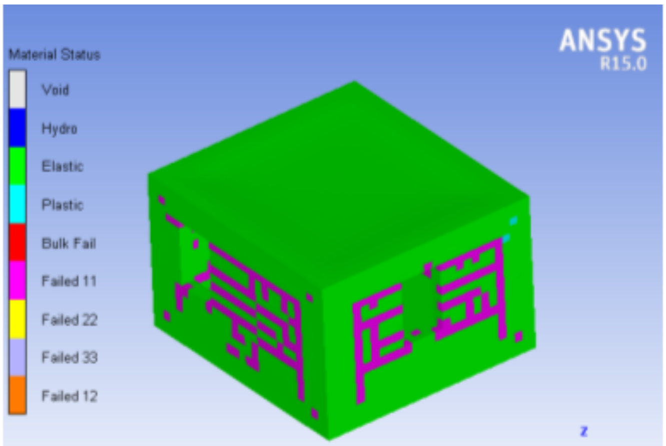

Figure 4. Damages detected in fill masonry s= 30 cm.

Damages are confined only in 30 cm thickness walls where fractures start to present openings of windows. Openings in model caused a localized increment of the blast wave velocity. The reinforced concrete part of structure is undamaged and stays in elastic field. The material failure is confined along the lateral and superior walls perimeter, where boundary conditions are strict and where there is an elements' stiffness variation. The damage is caused by bending failure of masonry elements.
In the second case the Gauges points are localized in the same position of the previous model. The blast pressure trend was differentiated in 30 cm and in 10 cm fill masonry.
In the first type of walls the hyperbolic diagram stays similar to the previous model because the blast load didn't cause an high strain rate (Figure 5). With 10 cm walls strains are very higher and for this reason depressions and over-pressures are very variable. The diagram generated can not be assimilable to an hyperbolic function because continuous reflection waves encountered in the room causing various peak pressures, with a less entity than the first peak of detonation.

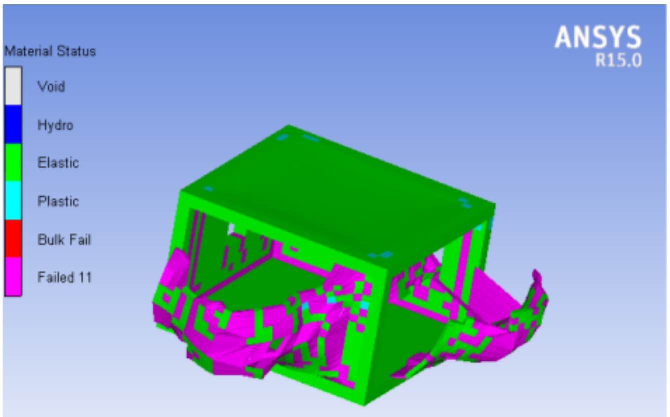

Figure 5. Damages detected in fill masonry s= 10-30 cm.

Smaller walls are the preferential element of rupture and so there is a minor damage of the main masonry. The damage is localized in superior and central area where the values of pressures are higher, causing the ejection of partitions and its total destruction. In corner area, where thicker walls encountered, the grade of damage is the same of the previously model. Bending failure material is determined by maximum strength value exceedance. In both cases RC frame didn't present a structural damage. For this reason it was studied an ulterior case where is reached the stechiometric saturation value in two room communicated.
The TNT equivalence was calculated with the same method of one room case. The stechiometric values of the LPG mixture the mass of TNT were reported in Table 6. Results obtained in this case were illustrated in Figure 6.

Table 6. TNT-LPG Equivalency two rooms.

Substance	Mass (kg)
LPG	4.84
TNT	1.51

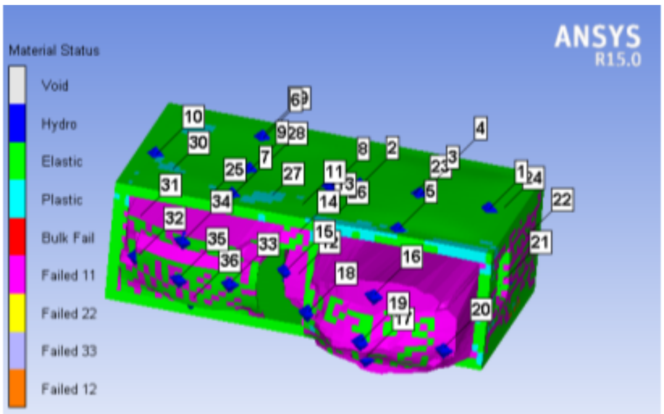

Figure 6. Damages detected in two saturated rooms communicated.

Also with two LPG saturated rooms there isn't damage in RC frame. However, the blast wave propagated in the adjacent room causes more damages only in no structural elements. Partition walls failures provide an outburst area that don't raise higher pressures in internal environmental compared to one room saturated. In the trigger room were ejected partition walls with an higher velocity than previously models.

6 CONCLUSION

The analyses performed highlight the invariance in thickness of partitions walls on RC frame damage.
This building type made with seismic-resistance technique is apt to resist to blast load too.
The results of this paper are to be considered overestimated because the TNT-equivalent mass method is usually utilized to study detonations while a LPG explosion is a deflagration.
The difference of two cases is both on duration of the phenomenon and on peak pressure values. In this paper, thermal effects that could be present in a blast load event, were not considered.
Actually, no specific software is present for an easy implementation of deflagration and for its interaction with structure elements of building.
Additional studies could be useful to investigate the thermal effects of LPG deflagration on structure elements. A future implementation of chemical deflagration formulas in a computational code software could allow the study of the phenomenon also in industrial environment where pressures and geometries cause turbulences that significantly affect consequences.

7 REFERENCES

Whittaker A.S., Sherkar P., 2010, Modeling the effects of detonations of high explosives to inform blast resistant design. MCEER, Buffalo, U.S.A.

Wang M., Hao H., Li Z., 2008, Prediction of fragment size and ejection distance of masonry wall under blast load using homogenized masonry material properties. Tianjin University, Tianjin, China

Fib Concrete, 2013, Model Code 2010 Volume 1. Fib International, Lusanne, Switzerland

ANSYS, 2009, Autodyn® User Manual Version 12.0. Ansys, Canonsburg, U.S.A.